Journal of Materials Chemistry A

Accepted Manuscript

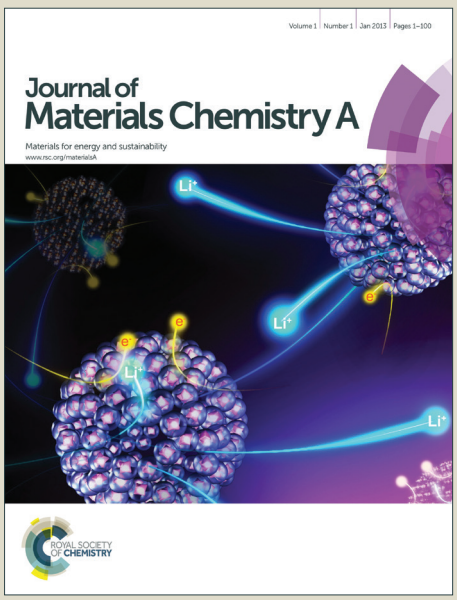

ROYAL SOCIETY OF CHEMISTRY

www.rsc.org/materialsA

Journal Name

ARTICLE

Improved stability of perovskite solar cells in ambient air by controlling mesoporous layer†

Received 00th January 20xx,
Accepted 00th January 20xx

DOI: 10.1039/x0xx00000x

www.rsc.org/

Jun Yin,[a,b] Jing Cao,[b] Xu He,[a] Shangfu Yuan,[b] Shibo Sun,[a] Jing Li,*[a,c] Nanfeng Zheng,*[b] and Liwei Lin[c]

Recently, organometal trihalide perovskite solar cells (PSCs) have gained intensive developing and show the huge potential as the next generation of high efficient photovoltaic (PV) cells. However, stability of the device still needs to be improved to satisfy the commercialization, especially the photovoltaic stability in ambient condition. In this work, the greatly improved stability of $CH_3NH_3PbI_3$ based PSCs in air ambient has been demonstrated by controlling the mesoporous TiO_2 (m-TiO_2) layer in the devices. With optimized thickness of m-TiO_2 layer, rather stable devices with maintaining over 85% of the initial power conversion efficiency (PCE) even after ~2400-hours (100 days) storage in air was accomplished. It is evidenced that the suppressed decomposition of perovskite and the well-kept charges transportation are majorly responsible for the improved device air-stability.

Introduction

Photovoltaic (PV) technology has been developed intensively in last decades with the goals towards high efficiency and low fabrication cost.[1] Since organometal trihalide perovskite was initially demonstrated as light sensitizer for photovoltaic cells by Miyasaka *et al* in 2009,[2] variety of studies have been done to improve the performance of the perovskite based solar cells, such as morphology control,[3-5] interface engineering,[5-8] crystal growth,[9-11] and so on. Recently, a new power conversion efficiency (PCE) record exceeding 20% has been certificated in the perovskite solar cells (PSCs).[12, 13] These attractive results make PSCs exhibit huge potential as the next generation high efficient solar cells with low cost fabrication processes.

Besides the pursuit of high efficiency, the stability of the PSCs is another crucial factor that determines their practicability. However, the most currently studied $CH_3NH_3PbI_xCl_{3-x}$ perovskite tends to degrade when exposed to air ambient,[14, 15] and the correspondingly produced PbI_2 grains sticking on the surface of the perovskite will block the carriers' efficient transportation and thus dramatically reduce the device's performance. Recently, a few works have focused on improving the stability of PSCs by introducing hydrophobic structure to prevent the moisture, such as carbon nanotube (CNT) combined with PMMA decoration,[16] aluminum oxide post-modification,[17] or using hydrophobic hole transporting layer[18, 19] and so on. Coincidentally, the widely used mesostructured scaffold materials in PSCs, such as TiO_2 and Al_2O_3, are also ideal protective architectures, which can be potentially utilized to protect the perovskite from moisture damage in air in some degree. Moreover, recently, the mesoporous TiO_2 also has been demonstrated the unique ability to increase the innate tolerance to environmental conditions due to its rapid electrons transporting property.[20] Therefore, the well-designed mesoporous TiO_2 structure is expected to help improve the photovoltaic stability of PSCs in air ambient, and the corresponding mechanisms are worth investigating.

In this work, by carefully controlling the thickness of mesoporous TiO_2 (m-TiO_2) layer in the PSCs, its impact on the device's performances, especially the stability in air ambient as well as the decay properties, have been systematically investigated. With the optimized m-TiO_2 thickness of 240 nm in the $CH_3NH_3PbI_3$ based PSCs, a quite stable performance with maintaining over 85% of the initial PCE was accomplished in the devices even after ~2400-hour (100 days) storage in air ambient. It is proposed and experimentally verified that the mesoporous TiO_2 layer not only can effectively prevent the damage of perovskite by moisture in air, but also provide a stable charge transportation channel, so that the photovoltaic performances of PSCs can be well maintained for a long time exposure to air ambient. This work well demonstrates the effect of the controllable mesoporous layer on improving the stability of $CH_3NH_3PbI_3$-based solar cells in air ambient, providing a specific guideline to realize air-stable PSCs.

Results and discussion

[a] Pen-Tung Sah Institute of Micro-Nano Science and Technology, Xiamen University, Xiamen, 361005, China. E-mail: lijing@xmu.edu.cn; Tel: +86-592-2181340.
[b] State Key Laboratory for Physical Chemistry of Solid Surfaces, Collaborative Innovation Center of Chemistry for Energy Materials, and Department of Chemistry, College of Chemistry and Chemical Engineering, Xiamen University, Xiamen 361005, China. E-mail: nfzheng@xmu.edu.cn; Fax: +86-592-2183047.
[c] Department of Mechanical Engineering, University of California, Berkeley, CA 94720, United States.

† Electronic Supplementary Information (ESI) available. See DOI: 10.1039/x0xx00000x

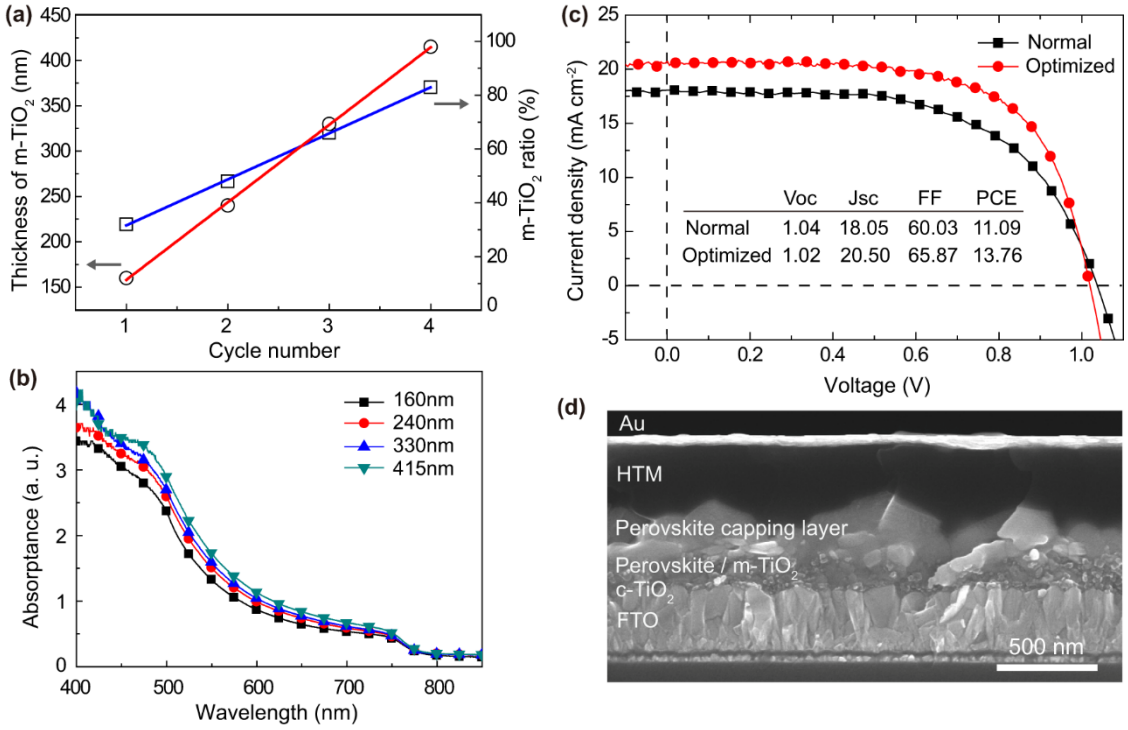

Fig. 1 (a) Statistics of the m-TiO_2 thickness and proportion to the total thickness of the active layer (m-TiO_2 ratio) by changing spin-coating cycles; and (b) the corresponding absorption spectra for the perovskite films with different m-TiO_2 thicknesses. (c) *J-V* curves for the as-prepared best-performing cells with and without optimization measured under simulated AM 1.5G solar irradiation of 100 mW cm^{-2}. The photovoltaic parameters extracted from *J-V* curves are summarized in inset. (d) Cross-sectional SEM micrographs of the best-performing solar cells.

Here, the solar cells were fabricated using the widely used two-step method[5, 21] and detailed fabrication processes can be seen in the Supporting Information (SI). All of the devices were fabricated under ambient air with humidity about 50% and then stored in dry air environment without sealing while maintaining the humidity of ~15% before measurements. The thickness of m-TiO_2 layer was controlled by employing different number of spin-coating cycles ranging from 1 to 4. As statistically shown in Figure 1a, the thickness of m-TiO_2 linearly increases with the cycle number, so does the m-TiO_2 ratio (defined as the ratio of the m-TiO_2-thickness to the total thickness of the active layer). From the cross-section images of the samples as shown in Figure S1, it can be found that the thickness of perovskite capping layer decreased as the m-TiO_2 increased, and total thickness of active layer maintained at ~500 nm without obvious variation. It is noteworthy that the perovskite crystal domains decreased due to the presence of thicker m-TiO_2 layer, consistent with Rietveld analysis reported previously.[22] The reduced size of perovskite grains would greatly influence the charge transportation process, which will be discussed later. The slightly increased absorption, as shown in Figure 1b, also indicates the change in the formation of perovskite sensitizer grains and the corresponding absorption kinetics by increasing the thickness of the mesoporous structure.[22]

The most efficient cells were realized on the devices configured by m-TiO_2 with the thickness of ~160 nm and achieved the PCE of 11.09% (10.43% in average). With optimized perovskite layer, 13.76% PCE (12.41% in average) can be obtained, as seen in the *J-V* curves of Figure 1c and histogram of efficiency in Figure S2 (SI). A well resolved perovskite capping layer with large crystal domains can be seen in this device (Figure 1d). It is believed that these large perovskite crystal domains insure the effective charges transportation processes and thus better photovoltaic performances. The comparison of reverse- and forward-scanning in *J-V* measurements also indicates that little hysteresis existed in the prepared devices (Figure S2c, SI). As the m-TiO_2 thickness increased, an obvious decreasing trend in open-circuit voltage (V_{oc}) can be observed, as well as the fill factor (FF) and PCE, while the short-circuit current density (J_{sc}) and incident photon-to-electron conversion efficiency (IPCE) response (Figure S3, SI) undergo a slight increase and then decrease, as shown in Figure 2.

In order to well understand the above phenomena, the electrochemical impedance spectra (EIS) measurement was performed to evaluate the charges recombination property in the PSCs. As shown in Figure S4a (SI), under full illumination and 1.0 V bias, the Nyquist plot showed typical arcs in the measured frequency range from 1 Hz to 1 MHz, which is attributed to the combination of the recombination resistance (R_{rec}) and the chemical capacitance (C_{μ}) of the considered film.[23] As shown in Figure S4b (SI), a distinguishable R_{rec} decreasing trend can be observed as the thickness of m-TiO_2

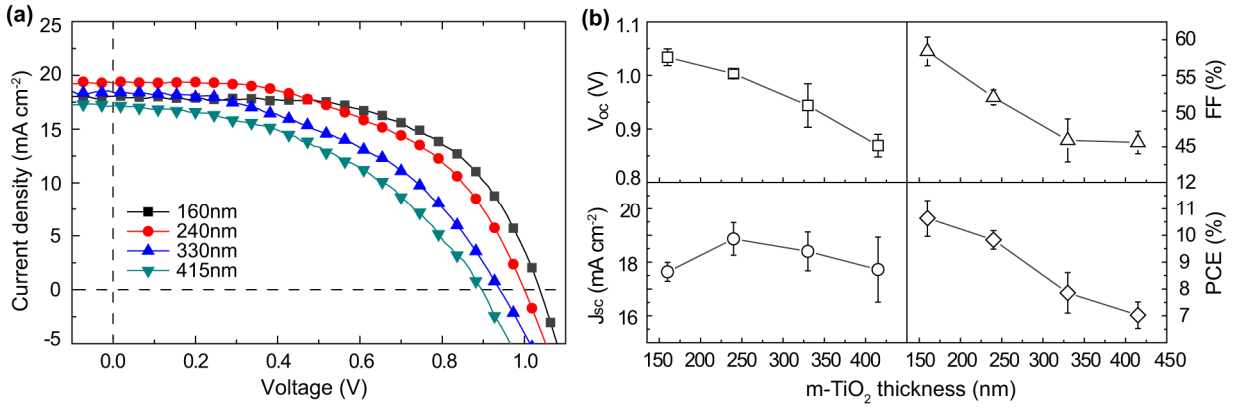

Fig. 2 (a) M-TiO$_2$-thickness dependence of the *J-V* characteristics under simulated AM 1.5G, 100 mW cm^{-2} irradiance; (b) The photovoltaic parameters extracted from *J-V* measurements of solar cells.

increased over the whole range of the applied voltages. This indicates that parasitic electron back reaction at the interface, especially between the mesoporous TiO_2 and the perovskite active layer, was enhanced with thickening m-TiO_2 layer due to the increased electron diffusion length.[7,24] This recombination reaction is known as the major loss factor for the V_{oc} decreasing in the devices originated from the reduced steady state electron density in the TiO_2 film.[25, 26] Also, the excess interfaces between TiO_2 and perovskite layer in thicker m-TiO_2 may bring extra trapping defects, which would quench the photo-generated carriers and lead to an increased series resistance (R_s), as presented as lowered FF. Additionally, the poorer charges transportation property with thickening m-TiO_2 layer resulted in an inefficient charges collection, leading to a slight increasing and then decreasing trend in J_{sc} and IPCE, although the absorption increased.

More importantly, the PCE decay measurements revealed that the mesoporous TiO_2 layer also plays an important role on the stability of the devices in air ambient, as displayed in Figure 3a and b. All the devices exhibit a PCE decay feature but with different trends. For the devices with thicker m-TiO_2 (240, 330 and 415 nm), the obvious decay happened on the first 7 days, and then a stable performance was maintained. In contrast, a continuous decay feature is presented in the devices with thinner m-TiO_2 layer (160 nm). Among all tested cells, the most efficient cells with 160-nm-m-TiO_2 layer present

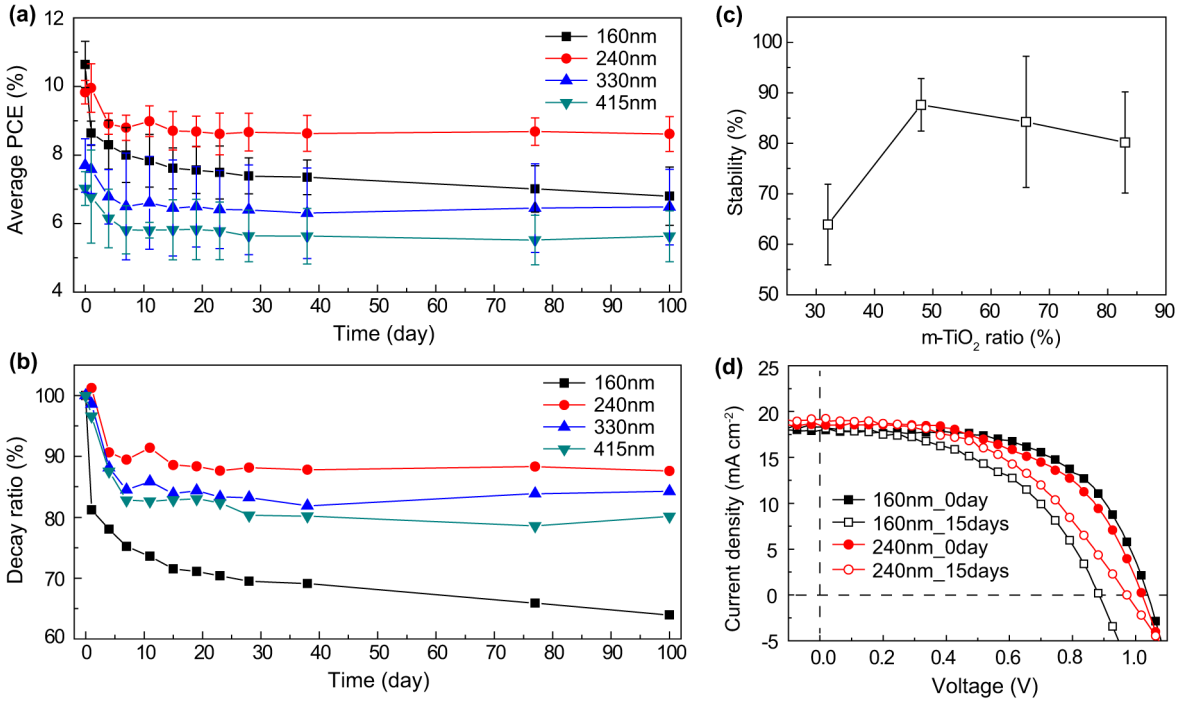

Fig. 3 (a) Long-term PCE stability measurement for the devices with controllable thickness of m-TiO_2 layer, and (b) the corresponding decay rate normalized to the initial PCE; (c) M-TiO_2-ratio dependent stability for the PSCs; (d) show the *J-V* curves for the typical devices with 160- and 240-nm-thick m-TiO_2 layer measured immediately and 15 days later, respectively. Average values of at least 6 samples or more with standard deviation are shown in (a).

Table 1 Summarized device parameters of PSCs with 160- and 240-nm-thick m-TiO_2 layer measured immediately and 15 days later.

Samples	V_{oc} (V)	J_{sc} (mA cm^{-2})	FF (%)	PCE (%)
160nm_0day	1.04	17.82	60.02	11.06
160nm_15days	0.88	18.09	48.36	7.72
240nm_0day	1.01	18.62	53.59	10.18
240nm_15days	0.97	18.95	47.28	8.72

a fastest decay rate. The cells with 240-nm-m-TiO_2 exhibit the best long-term stability. About 30% PCE loss occurred on the devices with 160-nm-thick of m-TiO_2 while only lower than 15% loss happened in the 240-nm ones even after about one month. To our surprise, the PCE for the devices with 240-nm-m-TiO_2 almost exhibit no more decay after the first 7 days and was maintained at the value about 9%. Even 100 days later, an average of ~8.61% (over 85% of initial average PCE value) and maximum of 9.15% PCE still can be obtained on these stable cells, as shown in Figure 3a and Figure S5 (SI). The device stability is evaluated by the ratio of the remaining PCE to its original value (decay ratio) after 100-day ageing, as illustrated in Figure 3c. Obviously, the stability of PSCs shows strong dependence on the proportion of m-TiO_2 layer within the active layer. The typical *J-V* curves of the corresponding cells measured immediately after fabrication and 15 days later also show similar decay features as the above (Figure 3d). The specific photovoltaic parameters summarized in Table 1 reveal that the decayed V_{oc} and FF are the main reasons for the apparent decreased PCE values on both kinds of the cells. Noticeable, the cells with 240-nm-thick m-TiO_2 layer are more stable because of the smaller V_{oc} and FF decreasing.

With fully considering the unique PV performances, EIS characteristics and long-term stability in air for the PSCs with different thicknesses of TiO_2, the relevant PV mechanisms is proposed as in Figure 4: for the perovskite solar cells employing thin m-TiO_2 layer, uniform film and large perovskite crystal domains can be produced, which enable the solar cells with good charges transportation and better photovoltaic performances,[11] as illustrated in Figure 4a. While for the cells configured with thicker mesoporous layer (as seen in Figure 4b), the reduced perovskite crystal domains and additionally introduced surface defects in the thick m-TiO_2 would result in a lower charge transportation rate, and thus a relative poorer PCE performances, exhibiting reduced V_{oc} and FF.

When experiencing a long exposure time to air, the cell structure with thin m-TiO_2 layer tends to be damaged by moisture in air, and the PbI_2 grains decomposed from perovskite would significantly limit the charges transportation processes (as illustrated in Figure 4c), leading to a dramatically decayed PCE performances. While for the sample with thicker m-TiO_2 layer (Figure 4d), the mesoporous structure intertwined with the perovskite can not only suppress the decomposition reaction of $CH_3NH_3PbI_3$ by preventing moisture attack in certain degree, but also ensure the charge transportation process to be well maitained.[20] So a relatively

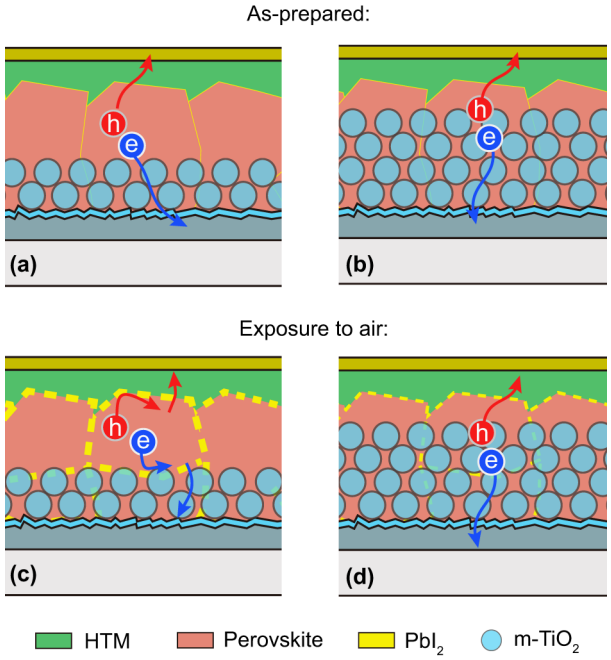

Fig. 4 Illustration of the cell's structure and charge transportation process with a (a) thin and (b) thick m-TiO_2 layer, respectively; (c) and (d) show the corresponding situation of the cells exposed to air for some time.

high PCE performance with the maximum of 9.15% and average of 8.61% in this work can be accomplished after the storage in air for 100 days, remaining more than 85% of its initial PCE, as shown in Figure S5 (SI).

To verify this decay mechanism, morphology characterization was first carried out to examine the evolution of perovskite film exposed to air ambient. As shown in Figure 5a, the as-prepared $CH_3NH_3PbI_3$ shows a typical cuboid crystal morphology with smooth surfaces and sharp edges.[11, 27] With the exposure time increasing, the surface changed to be rough and cuboid shape disappeared gradually, especially for the sample stored in air for over 30 days. Undoubtedly, the decomposition of perovskite and correspondingly produced PbI_2 grains on the surface should be the main reasons for the morphology evolution. The cross-sectional SEM images in Figure 5b and c show a clear m-TiO_2 layer dependent morphology evolution trends: in the newly prepared perovskite films for both of the samples with 160 and 240 nm-thick-m-TiO_2 layer, dense and large perovskite crystal domains can be seen presenting good consistence with the planar SEM images as shown in Figure 5a-i. After exposure to air for 15 days, the crystal size of the perovskite in both samples undergone an obvious decrease and the surface also became rough. Undoubtedly, the decomposition of perovskite film and generated PbI_2 nanograins adhering on the surface are the main reasons for this morphology evolution.[15] Differently, a much denser morphology in the perovskite bilayer was presented on the sample with thicker m-TiO_2 (240 nm) layer as seen in Figure 5c-ii. Then, as the exposure time further increasing to over 30 days, the crystal domains continuously

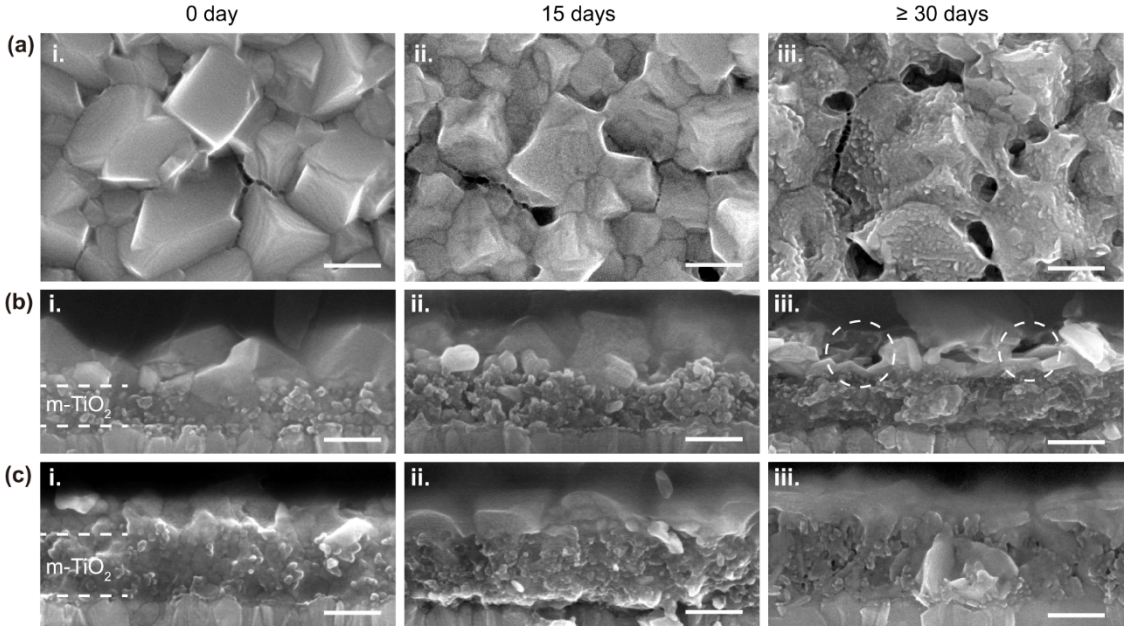

Fig. 5 Morphology evolution of the perovskite film as the exposure time increasing: (a) the surface SEM images of the perovskite films stored in air for (i.) 0 day, (ii.) 15 days and (iii.) 30 days, respectively; the cross-sectional SEM images of the perovskite films in completed PSCs devices with m-TiO_2 thickness of (b) 160 nm and (c) 240 nm that stored in air for 0 day (i.), 15 days (ii.) and over 30 days (about 40 days) (iii.) separately. Scale bar represents 200 nm.

decreased in size and obvious voids can be seen in the perovskite layer of the sample with thin m-TiO_2 layer of 160 nm. Certainly, these voids were formed from the seriously decomposed perovskite films, which would cause the detaching of the perovskite structure and then dramatically decrease the PV performances of PSCs.[15, 28] While for the sample with thicker m-TiO_2 layer (240 nm), better situation can be visualised in the cross-sectional image where relative denser and better collection between the charges collection layer still can be maintained after a long aging time in air, as shown in Figure 5c-iii.

The crystallinity evolutions as shown in Figure 6 further evidence the production of PbI_2 grains. The main diffraction peaks centred at 14.2° and 28.5° can be assigned to the $CH_3NH_3PbI_3$ phase, and the peak centred at 12.7° is attributed to PbI_2. For the as-prepared samples, both strong diffraction from perovskite and accompanied weak PbI_2 diffraction are present. The perovskite diffraction peak intensity also seems stronger for the sample with a thinner mesoporous layer, which should originate from the relatively thicker perovskite capping layer consisting of larger crystal domains compared with the samples with thick m-TiO_2 layer. For the samples stored in air for 15 days, the corresponding diffraction of the perovskite understandably decayed accompanied with the PbI_2 peak increasing in the intensity, as shown in Figure 6b, which is resulting from the decomposition reaction caused by the moisture in air. Interestingly, the XRD diffraction peaks undergo a quite unique decline trend for these samples, where more intensity reduction in perovskite related diffractions happened on the cells with thinner m-TiO_2 layer and the PbI_2 diffraction peaks experience a contrary trend. Furtherly, almost no changes occurred for the cell with 415-nm-thick m-TiO_2 layer, presenting as the most stable structure.

These characterization results indicate that the emerged PbI_2 grains, mainly located at the surface and grain boundary of perovskite, are the major defects in perovskite film when exposed to air for some time. And these defects would dramatically damage the interfaces between perovskite and charges conducting layer. Although the well-controlled PbI_2 boundary grains (GB) have been demonstrated to passive

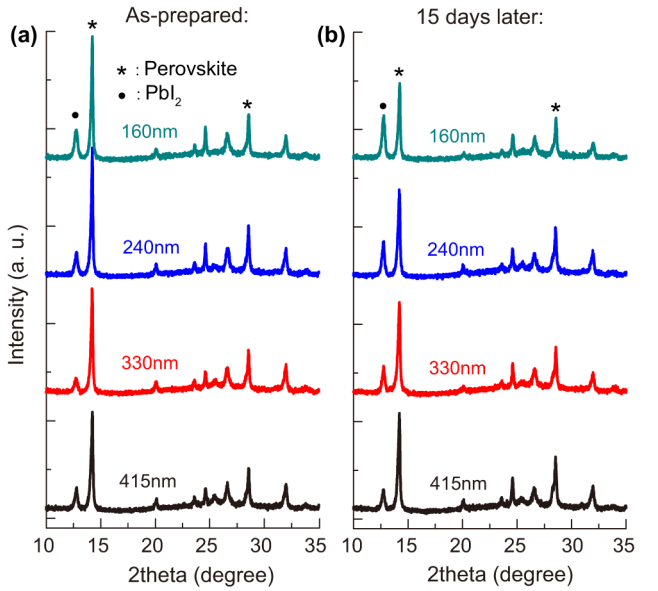

Fig. 6 XRD patterns corresponding to the perovskite film with controllable different thicknesses of m-TiO_2 layer (a) as-prepared and (b) stored in air for 15 days.

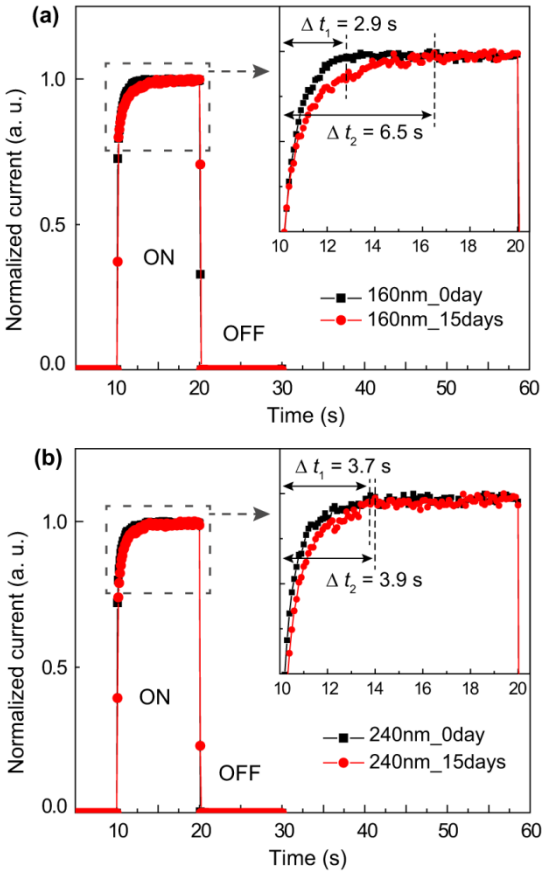

Fig. 7 Current dynamics for the typical devices with 160 and 240-nm-thick m-TiO_2 layer measured (a) immediately and (b) after 15-day storage in air. The inset is a zoom of the current rising region.

perovskites layer to achieve high PSCs performance,[29] the excess PbI_2 would still significantly block the charges transportation resulting in a lowered photovoltaic performances. So, there must be a compromise in the thickness of m-TiO_2 layer in order to: in one hand, suppress the electrons recombination reaction, and on the other hand reduce the production of PbI_2 grains due to the moisture attack, so that an efficient charge transportation process can be ensured in the well protected crystal structure and interfaces of the PSCs. Therefore, the optimized thickness of m-TiO_2 in 240 nm was demonstrated in the PSCs to achieve the satisfied performances in both conversion efficiency and stability.

In order to further demonstrate the influence of emerged PbI_2 grains on the charge transportation properties, current dynamics were investigated for the cells as-prepared and stored in air after 15 days by switching the light ON and OFF, as shown in Figure 7a and b. For the as-prepared cell with 160-nm-thick m-TiO_2 layer, a fast current response can be obtained with a short response time Δt_1 (2.9 s) when exposed under light, while a dramatically enlarged continuous current rise time Δt_2 (6.5 s) can be seen for the same cell that stored in air for 15 days. This indicates that the excessive charge accumulation at the electronic defect states occurred in the interfaces between TiO_2 / perovskite / HTM layers,[30] which would block the charges' efficient transportation and lead to a poorer photovoltaic performances, as demonstrated in Figure 3d. However, for the cells with relatively thicker m-TiO_2 layer of 240 nm, few changes can be visualized when comparing the current responses of the cell measured immediately and 15 days later, evidencing the not-too-much influenced charges transportation mechanism. Therefore, no prominent performance fading can be found on this device configuration. This conclusion is also further supported by time-resolved photoluminescence (TRPL) measurements as shown in Figure S5.

Conclusions

In this work, the mesoporous layer in perovskite solar cells has been demonstrated with specific functionality on enhancing the device's stability in air ambient while still maintaining the relatively satisfactory photovoltaic performances. With optimized thickness of m-TiO_2 layer, stable and efficient perovskite solar cells fabricated and stored in air ambient can be produced, which still maintain over 85% of its initial PCE value even after over 100-day exposure to air. The obviously enhanced stability in air for the perovskite solar cells is proposed to originate from the protected crystallinity and charge transportation channels induced by the relative thick mesoporous layer, which not only acts as a protective architecture, but also a stable electron transportation medium. The attractive results in this work not only reveal the specific influences of mesoporous structure on charge transportation and photovoltaic stability within perovskite solar cells in air ambient, but also provide a constructive way to fabricate efficient and stable perovskite solar cells by introducing or designing new mesoporous structures and configurations.

Acknowledgements

This work is financially supported by the National Natural Science Foundation of China (Grant No. 61106118), Science and Technology Program of Public Wellbeing of Xiamen City of China (3502Z20144079) and the China Scholarship Council (CSC) scholarship under the State Scholarship Fund.

Notes and references

‡ Footnotes relating to the main text should appear here. These might include comments relevant to but not central to the matter under discussion, limited experimental and spectral data, and crystallographic data.

1. M. A. Green, A. Ho-Baillie and H. J. Snaith, *Nature Photon.*, 2014, **8**, 506-514.
2. A. Kojima, K. Teshima, Y. Shirai and T. Miyasaka, *J. Am. Chem. Soc.*, 2009, **131**, 6050-6051.
3. A. Dualeh, N. Tétreault, T. Moehl, P. Gao, M. K. Nazeeruddin and M. Grätzel, *Adv. Funct. Mater.*, 2014, **24**, 3250-3258.
4. G. E. Eperon, V. M. Burlakov, P. Docampo, A. Goriely and H. J. Snaith, *Adv. Funct. Mater.*, 2014, **24**, 151-157.

5. J. Burschka, N. Pellet, S. J. Moon, R. Humphry-Baker, P. Gao, M. K. Nazeeruddin and M. Gratzel, *Nature*, 2013, **499**, 316-319.
6. H. Zhou, Q. Chen, G. Li, S. Luo, T. B. Song, H. S. Duan, Z. Hong, J. You, Y. Liu and Y. Yang, *Science*, 2014, **345**, 542-546.
7. M. M. Lee, J. Teuscher, T. Miyasaka, T. N. Murakami and H. J. Snaith, *Science*, 2012, **338**, 643-647.
8. M. Liu, M. B. Johnston and H. J. Snaith, *Nature*, 2013, **501**, 395-398.
9. W. Nie, H. Tsai, R. Asadpour, J. C. Blancon, A. J. Neukirch, G. Gupta, J. J. Crochet, M. Chhowalla, S. Tretiak, M. A. Alam, H. L. Wang and A. D. Mohite, *Science*, 2015, **347**, 522-525.
10. D. Shi, V. Adinolfi, R. Comin, M. Yuan, E. Alarousu, A. Buin, Y. Chen, S. Hoogland, A. Rothenberger, K. Katsiev, Y. Losovyj, X. Zhang, P. A. Dowben, O. F. Mohammed, E. H. Sargent and O. M. Bakr, *Science*, 2015, **347**, 519-522.
11. J. H. Im, I. H. Jang, N. Pellet, M. Gratzel and N. G. Park, *Nature Nanotechnol.*, 2014, **9**, 927-932.
12. National Renewable Energy Laboratory, Best Research-Cell Efficiencies; www.nrel.gov/ncpv/images/efficiency_chart.jpg.
13. W. S. Yang, J. H. Noh, N. J. Jeon, Y. C. Kim, S. Ryu, J. Seo and S. I. Seok, *Science*, 2015, **348**, 1234-1237.
14. J. L. Yang, B. D. Siempelkamp, D. Y. Liu and T. L. Kelly, *ACS nano*, 2015, **9**, 1955-1963.
15. Y. Han, S. Meyer, Y. Dkhissi, K. Weber, J. M. Pringle, U. Bach, L. Spiccia and Y.-B. Cheng, *J. Mater. Chem. A*, 2015, **3**, 8139-8147.
16. S. N. Habisreutinger, T. Leijtens, G. E. Eperon, S. D. Stranks, R. J. Nicholas and H. J. Snaith, *Nano Lett.*, 2014, **14**, 5561-5568.
17. G. Niu, W. Li, F. Meng, L. Wang, H. Dong and Y. Qiu, *J. Mater. Chem. A*, 2014, **2**, 705-710.
18. L. Zheng, Y.-H. Chung, Y. Ma, L. Zhang, L. Xiao, Z. Chen, S. Wang, B. Qu and Q. Gong, *Chem. Commun.*, 2014, **50**, 11196-11199.
19. Y. S. Kwon, J. Lim, H.-J. Yun, Y.-H. Kim and T. Park, *Energy Environ. Sci.*, 2014, **7**, 1454-1460.
20. F. T. F. O'Mahony, Y. H. Lee, C. Jellett, S. Dmitrov, D. T. J. Bryant, J. R. Durrant, B. C. O'Regan, M. Graetzel, M. K. Nazeeruddin and S. A. Haque, *J. Mater. Chem. A*, 2015, **3**, 7219-7223.
21. K. Liang, D. B. Mitzi and M. T. Prikas, *Chem. Mater.*, 1998, **10**, 403-411.
22. L. Wang, C. McCleese, A. Kovalsky, Y. Zhao and C. Burda, *J. Am. Chem. Soc.*, 2014, **136**, 12205-12208.
23. A. Dualeh, T. Moehl, M. K. Nazeeruddin and M. Gratzel, *ACS nano*, 2013, **7**, 2292-2301.
24. Y. Zhao and K. Zhu, *J. Phys. Chem. L.*, 2013, **4**, 2880-2884.
25. A. K. Chandiran, A. Yella, M. T. Mayer, P. Gao, M. K. Nazeeruddin and M. Gratzel, *Adv Mater*, 2014, **26**, 4309-4312.
26. D. Bi, L. Yang, G. Boschloo, A. Hagfeldt and E. M. J. Johansson, *J. Phys. Chem. L.*, 2013, **4**, 1532-1536.
27. T. Baikie, Y. Fang, J. M. Kadro, M. Schreyer, F. Wei, S. G. Mhaisalkar, M. Graetzel and T. J. White, *J. Mater. Chem. A*, 2013, **1**, 5628.
28. B. Conings, J. Drijkoningen, N. Gauquelin, A. Babayigit, J. D'Haen, L. D'Olieslaeger, A. Ethirajan, J. Verbeeck, J. Manca, E. Mosconi, F. D. Angelis and H.-G. Boyen, *Adv. Energy Mater.*, 2015, DOI: 10.1002/aenm.201500477, n/a-n/a.
29. Q. Chen, H. Zhou, T.-B. Song, S. Luo, Z. Hong, H.-S. Duan, L. Dou, Y. Liu and Y. Yang, *Nano Lett.*, 2014, **14**, 4158-4163.
30. H. S. Kim, I. Mora-Sero, V. Gonzalez-Pedro, F. Fabregat-Santiago, E. J. Juarez-Perez, N. G. Park and J. Bisquert, *Nature Commun.*, 2013, **4**, 2242.

Graphical Abstract for:

Improved stability of perovskite solar cells in ambient air by controlling mesoporous layer

Jun Yin,[a,b] Jing Cao,[b] Xu He,[a] Shangfu Yuan,[a] Shibo Sun,[a] Jing Li,[*a,c] Nanfeng Zheng,[*b] and Liwei Lin[c]

Recently, organometal trihalide perovskite solar cells (PSCs) have gained intensive developing and show the huge potential as the next generation of high efficient photovoltaic (PV) cells. However, stability of the device still needs to be improved to satisfy the commercialization, especially the photovoltaic stability in ambient condition. In this work, the greatly improved stability of $CH_3NH_3PbI_3$ based PSCs in air ambient has been demonstrated by controlling the mesoporous TiO_2 (m-TiO_2) layer in the devices. With optimized thickness of m-TiO_2 layer, rather stable devices with maintaining over 85% of the initial power conversion efficiency (PCE) even after ~2400-hours (100 days) storage in air was accomplished. It is evidenced that the suppressed decomposition of perovskite and the well-kept charges transportation are majorly responsible for the improved device air-stability.

Table of contents Figure:

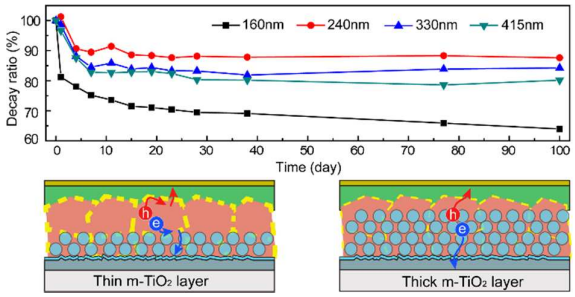

With optimized thickness of m-TiO_2 layer, rather stable perovskite solar cells with maintaining over 85% of the initial power conversion efficiency (PCE) even after 100-day storage in air was accomplished.